CHEMISTRY OF MATERIALS
Article

Chem. Mater. **2009,** *21,* 2727–2732 2727
DOI:10.1021/cm900265q

Novel High-Performance Liquid-Crystalline Organic Semiconductors for Thin-Film Transistors

Ping Liu,*[,†,‡] Yiliang Wu,[†] Hualong Pan,[†,§] Yuning Li,[†,§] Sandra Gardner,[†] Beng S. Ong,[†,⊥,§] and Shiping Zhu*[,‡]

[†]*Xerox Research Centre of Canada, Mississauga, Ontario, Canada L5K 2L1, and* [‡]*Department of Chemical Engineering, McMaster University, Ontario, Canada L8S 4L7.* [§] *Current address: Institute of Materials Research and Engineering, Singapore 117602.* [⊥] *Current address: School of Materials Science & Engineering, Nanyang Technological University, Singapore 639798.*

Received January 28, 2009. Revised Manuscript Received May 7, 2009

A novel class of liquid-crystalline organic semiconductors based on 2,5′-bis-[2-(4-pentylphenyl)vinyl]-thieno(3,2-*b*)thiophene and 2,5′-bis-[2-(4-pentylphenyl)vinyl]-(2,2′)bithiophene were synthesized through proper structural design. The materials exhibited high field-effect mobilities up to 0.15 $cm^2\ V^{-1}\ s^{-1}$ and current on/off ratio of 1×10^6. The high performance is attributed to their abilities to form highly ordered structures through molecular packing, which is revealed by single-crystal and thin film X-ray diffraction (XRD). The structures were analyzed by polarized optical microscope and showed obvious changes in texture corresponding to the phase changes in DSC diagrams, indicating their abilities to form liquid-crystalline structures. High environmental stabilities have been demonstrated with these new compounds, which is consistent with their low HOMO levels and large band gaps. In addition, UV−vis spectra of the thin films formed from these compounds have showed that their absorption peaks mainly appear in the range of ultraviolet spectrum region, indicating they could be used for the application of those circuits requiring transparency such as optoelectronic devices.

Introduction

Organic thin-film transistors (OTFTs) have attracted great interests in both industrial and academic research communities as low-cost alternatives to traditional silicon-based transistors for electronic applications in the past two decades.[1−6] OTFTs are particularly attractive for large-area electronic device applications where high processing speeds are not required, such as backplane electronics for large displays, electronic paper and radio frequency identification (RFID) tags, etc. For these applications, it is critical that the organic semiconductor materials have sufficient stabilities in ambient conditions with high OTFT performance in order to achieve low-cost manufacturing processes and high OTFTs stabilities. However, very few organic semiconductor materials possess both high mobility and environmental stability. Most high performance p-type organic semiconductors such as pentacenes, polythiophenes, and their derivatives[7,8] have relatively high HOMOs and small band gaps and therefore they are easily oxidized when processed or operated in ambient conditions, resulting in significant degradation in performance. The lack of environmental stability of these organic semiconductor materials presents great challenges for the low-cost manufacturing processes where ambient conditions are preferred. It also limits the OTFT applications where light emission such as backlight is involved. Recently, several stable and high performance organic OTFTs based on oligofluorene derivatives,[9a,9b] thiophene-phenylene, thiophen-thiazole oligomers,[10a−10d]

*Corresponding author. E-mail: ping.liu@xrcc.xeroxlabs.com (P.L.); zhuship@mcmaster.ca (S.Z.).

(1) Garnier, F.; Hajlaoui, R.; Yassar, A.; Srivastava, P. *Science* **1994**, *265*, 1684.
(2) Bao, Z. *Adv. Mater.* **2000**, *12*, 227.
(3) Dimitrakopoulos, C. D.; Mascaro, D. J. *Adv. Mater.* **2002**, *14*, 99.
(4) (a) Sirringhaus, H.; Tessler, N.; Friend, R. H. *Science* **1998**, *280*, 1741. (b) Sirringhaus, H.; Brown, P. J.; Friend, R. H.; Nielen, M. M.; Bechgaard, K.; Langeveld-Voss, B. M. W.; Spiering, A. J. H.; Janssen, R. A. J.; Meijer, E. W.; Herwig, P.; de Leeuw, D. M. *Nature* **1999**, *401*, 685.
(5) Katz, H. E. *Chem. Mater.* **2004**, *16*, 4748.
(6) Singh, T. B.; Sariciftci, N. S. *Annu. Rev. Mater. Res.* **2006**, *36*, 199.
(7) (a) Afzali, A.; Dimitrakopoulos, C. D.; Breen, T. L. J. *Am. Chem. Soc.* **2002**, *124*, 8812. (b) Kelly, T. W.; Boardman, L. D.; Dunbar, T. D.; Muyres, D. V.; Pellerite, M, J.; Smith, T. P. *J. Phys. Chem. B* **2003**, *107*, 5877. (c) Sundar, V. C.; Zaumseil, J.; Podzorov, V.; Menard, E.; Willett, R. L.; Someya, T.; Gershenson, M. E.; Rogers, J. A. *Science* **2004**, *303*, 1644.
(8) (a) Bao, Z.; Dodabalapur, A.; Lovinger, A. J. *Appl. Phys. Lett.* **1996**, *69*, 4105. (b) Sirrignhaus, H.; Tessler, N.; Friend, R. H. *Science* **1998**, *280*, 1741. (c) Ong, B. S.; Wu, Y.; Liu, P.; Gardner, S. *J. Am. Chem. Soc.* **2004**, *126*, 3378. (d) Mcculloch, I; Heeney, M.; Bailey, C.; Genevicius, K.; Macdonald, I.; Shkunov, M.; Sparrowe, D.; Tierney, S.; Wagner, R.; Zhang, W.; Chabinyc, M. L.; Kline, R. J.; Mcgehee, M. D.; Toney, M. F. *Nat. Mater.* **2006**, *5*, 328.
(9) (a) Meng, H.; Bao, Z.; Lovinger, A. J; Wang, B. C.; Mujsce, A. M. *J. Am. Chem. Soc.* **2001**, *123*, 9214. (b) Locklin, J.; Ling, M. M.; Sung, A.; Roberts, M. E.; Bao, Z. *Adv. Mater.* **2006**, *18*, 2989.
(10) (a) Hong, X. M.; Katz, H. E.; Lovinger, A. J.; Wang, B. C.; Raghavachari, K. *Chem. Mater.* **2001**, *13*, 4686. (b) Mushrush, M.; Facchetti, A.; Lefenfeld, M.; Katz, H. E.; Marks, T. J. *J. Am. Chem. Soc.* **2003**, *125*, 9414. (c) Katz, H. E.; Siegrist, T.; Lefenfeld, M.; Gopalan, P.; Mushrush, M.; Ocko, B.; Gang, O.; Jisrawl, N. *J. Phys. Chem. B* **2004**, *108*, 8567. (d) Sung, A.; Ling, M. M.; Tang, M. L.; Bao, Z.; Locklin, J. *Chem. Mater.* **2007**, *19*, 2342.

Published on Web 06/17/2009

Scheme 1. Syntheses of New Organic Semiconductors 7 and 8

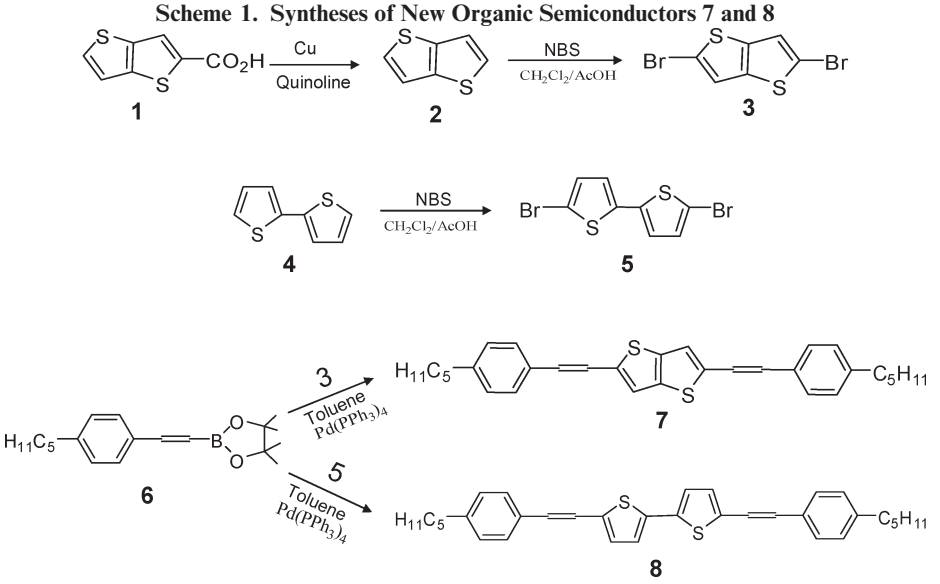

and antracene-based compounds[11] have been reported. Thiophene and thienothiophene-based polythiophenes have received great attention for the OTFT application because of their high mobilities.[8c,8d] However, like most highly conjugated polythiophenes, they are not very stable in air. In this article, we report our studies on a new class of semiconductors based on the molecular structures of 2,5′-bis-[2-(4-pentylphenyl)vinyl]-thieno(3,2-*b*)thiophene **7** and 2,5′-bis-[2-(4-pentylphenyl)vinyl]-2,2′-bithiophene **8**, which exhibit high OTFT performance with remarkable air stability.

Results and Discussion

New semiconductors **7** and **8** were synthesized according to the procedure shown in Scheme 1. Thieno[3,2-*b*]-thiophene-2-carboxylic acid **1** was prepared accordingly by following a synthetic method published in the literature.[12] Compound **2** was obtained with 90% yield by refluxing **1** in quinoline with copper powder. Compounds **3** and **5** were prepared by bromination of **2** and **4** with *N*-bromosuccinimide (NBS) in a mixture of dichloromethane and acetic acid at room temperature, respectively. Compounds **7** and **8** were synthesized via Suzuki coupling from the commercially available compound **6** with **3** and **5**, respectively, in good yields (> 65%).

The UV−vis spectra of compound **7** and **8** in chlorobenzene solution and their thin films on glass are shown in Figure 1. The absorption spectra of **7** and **8** in chlorobenzene solution have their λ_{max} value at 410 and 432 nm, respectively. The absorption spectra of vacuum-deposited thin films of **7** and **8** have the absorption maxima (λ_{max}) at 345 and 351 nm, respectively, which indicate larger band gaps than most organic semiconductors, especially

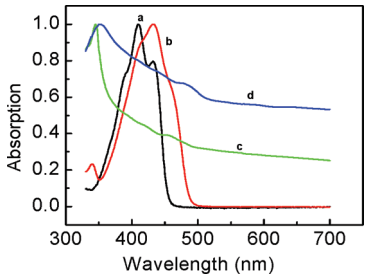

Figure 1. UV−vis spectra of compounds **7** and **8**. a and b represent **7** and **8** in chlorobenzene solution, respectively; c and d represent their thin films of **7** and **8** on glass substrates, respectively.

compared to acenes and their derivatives.[7,8,11,13] Semiconductors of this nature without absorption in the visible region are particularly suitable for transparent OTFTs that can be used in those circuits requiring transparency such as optoelectronic devices.[14,15] The cyclic voltammetric measurements of **7** and **8** showed a reversible oxidation process with similar onset oxidation potential at 0.80−0.82 eV against Ag/AgCl electrode, which corresponds to an estimated HOMO level (ionization potential) of 5.18−5.20 eV from vacuum (see the Supporting Information). Thus both UV−vis and cyclic voltammetric spectra indicate their high stabilities against oxidation in ambient conditions.

Molecular packing of compound **8** was investigated with single-crystal XRD. As shown in Figure 2, the two thiophene rings in the center are coplanar with a torsional angle of 180° (C3−C2−C2′−C3′). The five-membered ring of thiophene also has less steric hindrance to the hydrogen atom attached to C6, which results in better coplanarity with a smaller torsional angle of 8.4° (C7−C6−C4−C5), compared with a counterpart torsional angle of 10.6° in a substituted anthracene system.[11] The

(11) (a) Meng, H.; Sun, F.; Goldinger, M. B.; Jaycox, G. D.; Li, Z.; Marshall, W. J.; Blackman, G. S. *J. Am. Chem. Soc.* **2005**, *127*, 2406. (b) Meng, H.; Sun, F.; Goldinger, M. B.; Gao, F.; Londono, D. J.; Marshal, W. J.; Blackman, G. S.; Dobbs, K. D.; Keys, D. E. *J. Am. Chem. Soc.* **2006**, *128*, 9304.
(12) Fuller, L. S.; Iddon, B.; Smith, K. A. *J. Chem. Soc., Perkin Trans.* **1997**, *1*, 3465.
(13) Li, Y.; Wu, Y.; Liu, P.; Prostran, Z.; Gardner, S.; Ong, B. S. *Chem. Mater.* **2007**, *19*, 418.
(14) Nomura, K.; Ohta, H.; Ueda, K.; Kamiya, T.; Hirano, M.; Hosono, H. *Science* **2003**, *300*, 1269.
(15) Wu, Y.; Li, Y.; Gardner, S.; Ong, B. S. *J. Am. Chem. Soc.* **2005**, *127*, 614.

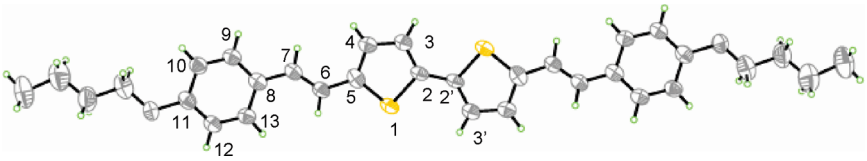

Figure 2. Thermal ellipsoid plots (prepared at the 30% probability level) of the single-crystal structure of **8** (viewed down the thiophene plane).

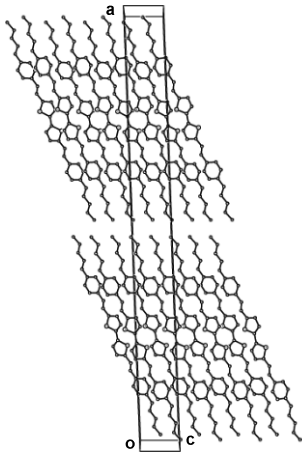

Figure 3. Schematic view of the molecular packing of compound **8** as seen down the *b*-axis. (Hydrogen atoms are not shown for clarity.).

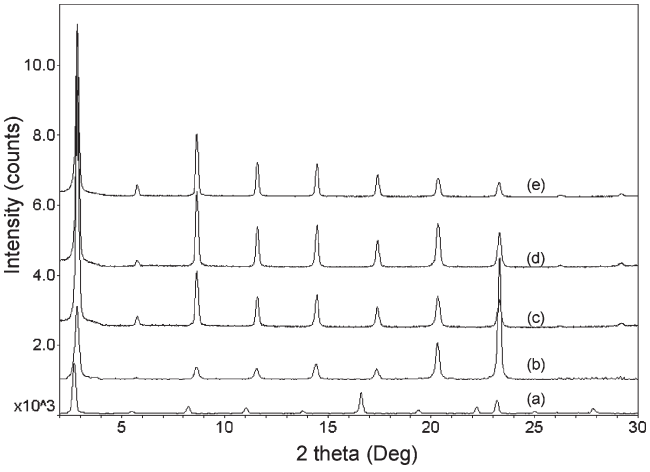

Figure 4. X-ray diffraction patterns of 100 nm thin films: (a) thin film of compound **8** at room temperature; (b−e) compound **7** with substrate temperature at room temperature, 40, 60, and 80 °C, respectively.

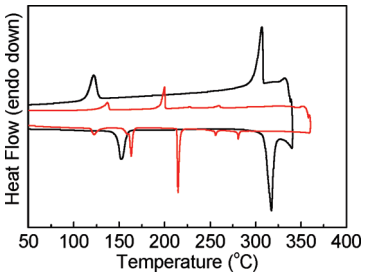

Figure 5. DSC thermograms of compound **7** and **8**. **7** (black line); **8** (red line).

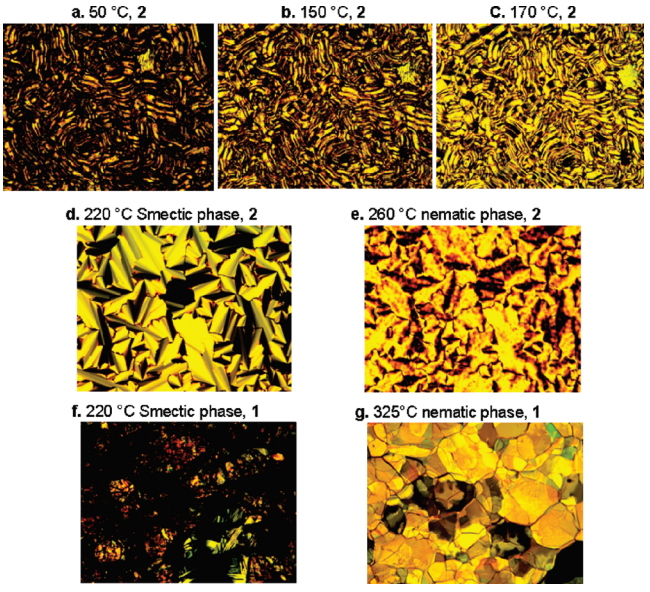

Figure 6. Polarized optical microscopic images of compound **8** at (a) 50, (b) 150, (c) 170, (d) 220, and (e) 260 °C, respectively; and compound **7** at (f) 220 and (g) 325 °C, respectively.

carbon (C6) in the molecule is in high planarity with maximum deviation of 0.45 Å from thiophene plane.

The linear structure of this class of molecules is facilitated by the trans-conformation of vinyl groups. Such elongated linear structure with a rigid segment in the central region and flexible chains in its two ends is a perfect example of a typical liquid-crystal molecule, which has been clearly observed in their three-dimensional arrangement of the molecules in the single crystal (Figure 3).

The strong anisotropic intermolecular forces from the aromatic $\pi-\pi$ interactions and the high ratio of length (~32.0 Å)/width (~3.0 Å) make the molecules align well with a lamellar structure. The interlayer distance derived from the peak at (200) is 32.1 Å, which is about the same as the molecule length. This means there is no interdigitation of alkyl chains between the layers, which favors the growth of large domain in the *b*, *c*-plane (parallel to the substrate surface). For compound **7**, where the central region of the molecule is a thieno[3,2-*b*]thiophene, the anisotropy of intermolecular force becomes larger and the relatively weak force between the layers results in poor periodicity of atoms between the layers. So only very strong interlayer refection points related with interlayer distance were found in the single crystal XRD measurement, indicating clear lamellar structures in the crystal, but no three-dimensional molecule ordering was solved.

The molecular ordering of compounds **7**, **8** in thin film was also studied using X-ray diffraction. Figure 4 shows the diffraction patterns of the thin films prepared at different substrate temperatures. The diffraction peak of compound **7** at 2θ of 2.88° corresponds to a *d*-spacing of 30.7 Å, which is the same as the extended molecular

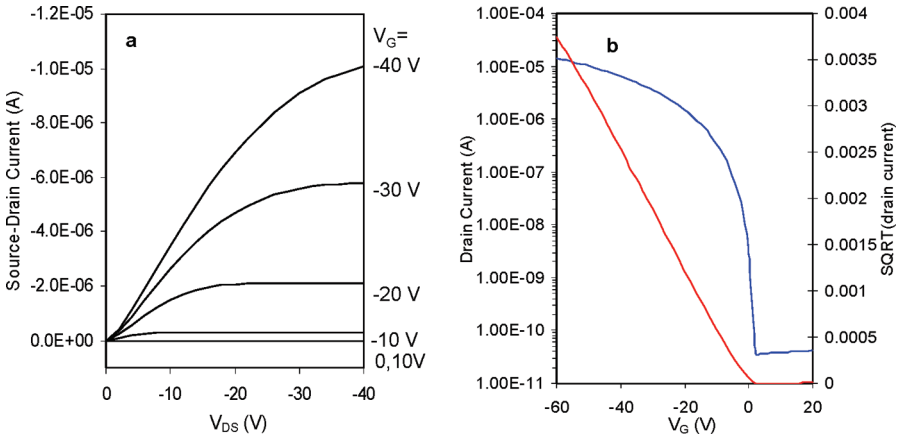

Figure 7. OTFTs characteristics of an exemplary with vacuum-deposited compounds **7** and **8** as channel semiconductors (substrate at 60 °C, channel length 90 μm and channel width 5000 μm): (a) Output curves at various gate voltages for compound **7**; (b) a transfer curve for compound **8** in the saturated regime at a constant $V_{DS} = -40$ V and the square root of the absolute value of the current as a function of the gate voltage.

length. It indicates that the molecules are aligned with their long axis normal to the substrate. The diffraction peaks up to eighth order could be observed, revealing a highly crystalline order of the vacuum deposited film. Compound **8** shows a diffraction peak at 2θ of 2.74°, which corresponds to a *d*-spacing of 32.2 Å. The *d*-spacing agrees to the interlayer distance obtained from the single crystal data.

The thermal properties of compound **7** and **8** were evaluated by DSC, as shown in Figure 5. The DSC thermograms show two endotherms at 152.6 and 321.9 °C for **7** (black line), and multiple peaks for 8 (129.3, 163.0, 214.7, 251, and 275 °C) (red line), indicating liquid-crystalline properties of the compounds. The phases are assigned and discussed in the following, together with polarized optical microscopy. The phase transition temperature from liquid crystalline to isotropic phase transition for **7** (321.9 °C) is much higher than that for **8** (214.7 °C). This result is consistent with their chemical structures as compound **7** has a rigid fused thieno[3,2-*b*]thiophene in its backbone.

The molecular organizations of both compounds **7** and **8** were further examined by polarized optical microscope. Both compounds experienced obvious texture changes at temperatures where the phase changes occurred in the DSC diagrams. For example, compound **8** gave Schlieren texture on cooling from the isotropic phase (Figure 6e), indicating it was in a nematic phase at 260 °C. On further cooling, a typical focal conic texture revealed the formation of a smectic A phase (Figure 6d). When cooled below 210 °C, a dramatic texture change was observed (Figure 6c), which probably represented a smectic C phase. On further cooling, although the texture was not changed, the brightness decreased according to each phase transition (Figure 6b and Figure 6a). For compound **7**, a typical mosaic texture was observed in the temperature range from 150 to 320 °C, indicating the formation of a smectic phase of the material (Figure 6f). Further study of these compounds using temperature-dependent X-ray diffraction will be conducted to understand the phase transitions.

To investigate their OTFT properties, we vacuum-deposited thin films (~100 nm) of compounds **7** and **8** on n^{++}-Si substrates as channel semiconductors in both top-contact and bottom-contact OTFT device configurations. The transfer and output characteristics of the devices indicated that both **7** and **8** are typical p-type semiconductors (Figure 7). The top-contact devices showed close to zero turn-on voltage and good saturation behavior with a small contact resistance. The characteristics of top-contact OTFTs comprised from *7* and **8** as the semiconductor layer at various substrate temperatures are summarized in Table 1. It was observed that the OTFT performances for both compounds depended on the temperature of the substrate. Good performance with the mobility up to 0.15 $cm^2 V^{-1} S^{-1}$ and on/off ratio of 1×10^6 was obtained when compound **7** was deposited at a substrate temperature of 60 °C. It was also noted that the field-effect mobility of **7** was much higher than that of **8** at both 60 °C and room temperature, which may be attributed to the more effective π conjugations and closer $\pi-\pi$ overlaps of compound **7**. Bottom contact devices with compounds **7** and **8** at the optimal substrate temperature showed saturated mobilities of 0.075 and 0.006 $cm^2/(V s)$, respectively, which is around a factor of 2 lower than those in top-contact devices. The decrease of mobility in bottom-contact configuration was reported for various semiconductors including pentacene and polythiophenes, which is attributed to the increased contact resistance in the bottom-contact configuration.

Table 1. Summary of OTFT Mobility and Current on/off Ratio with Compounds 7 and 8 as Semiconductor at Various Substrate Temperatures

sample	substrate temp (°C)	mobility ($cm^2/(V s)$)	on/off ratio
7	r.t.	0.05−0.06	10^5 to 10^6
7	40	0.077−0.081	10^5 to 10^6
7	60	0.1−0.15	10^6
7	80	0.0004−0.002	10^3 to 10^5
8	r.t.	0.01−0.02	10^5 to 10^6
8	40	0.01−0.02	10^6
8	60	0.039−0.053	10^5 to 10^6
8	80	0.023−0.030	10^6

The effect of the substrate temperature on the device mobility was also evident from the X-ray diffraction (XRD) data. As shown in Figure 4, the peak intensities

increased gradually as the substrate temperature increased from room temperature to 60 °C, indicating that the order of molecular structure in the film was improved, and thus the increased mobility was resulted. The decrease in mobility with further increasing substrate temperature from 60 to 80 °C for both compounds was probably due to pronounced grain boundary in the thin film with large crystals in size, because the orientation of molecules in the thin film was not changed as indicated by the same diffraction patterns. It should be noted that all devices were characterized at room temperature. Studies on device performance at elevated temperatures such as the liquid-crystalline phase transition temperatures are underway.

Consistent with the properties of low HOMO level and large band gaps of this class of organic semiconductor, OTFT devices with these compounds exhibited excellent air stability. When stored in the dark in ambient air for 2 years, the device with compound 7 showed a mobility of 0.077 $cm^2/(V\ s)$, only a factor of 2 lower than that of the fresh device (see Figure S2 in the Supporting Information). This high stability feature may enable practical application of this class of organic semiconductors.

Conclusion

In conclusion, a new class of high-performance liquid crystalline p-type organic semiconductors has been developed for OTFT applications. Our results revealed that this class of organic semiconductors has a strong tendency to form highly ordered molecular structures with liquid-crystalline characteristics, which contributes to their good performance in the OTFT devices. These new organic semiconductors have both lower HOMO levels and larger band gaps than the most other p-type organic semiconductors such as acenes, polythiophenes, and their derivatives. Excellent environmental stabilities have been demonstrated for the OTFT devices comprised from these semiconductor materials. In addition, these new organic semiconductors have a great potential for those electronic device applications where transparent OTFTs are required because their thin film absorption peaks appear mainly in the range of ultraviolet spectrum region.

Experimental Procedures

Instrumentations and Measurements. NMR spectra were obtained in $CDCl_3$ with a Bruker DPX 300 NMR spectrometer with tetramethylsilane as an internal reference. Absorption spectra were measured on a Varian Cary-5 UV−vis−NIR Spectrophotometer for both thin films and chlorobenzene solutions. DSC thermograms were obtained on TA Instruments DSC 2910 differential scanning calorimeter with a heating rate of 10 °C per minute under nitrogen atmosphere. The single crystal of **8** for structure analysis was grown by recrystallization from a mixture solvent of toluene and chlorobenzene at a ratio of three to one by volume. Single-crystal X-ray diffraction was performed on a Bruker Smart 6000 CCD 3-cicle D8 diffractometer with a Cu RA X-ray source (λ = 1.5418 Å) at room temperature. Thin film X-ray diffraction was performed on a Rigaku MiniFlex spectrometer using a Cu X-ray source at room temperature. Cyclic voltammetric measurements were carried out on a BAS 100 voltammetric system with a three electrode cell in a solution of tetrabutylammonium perchlorate, Bu_4NClO_4, in dichlormethane (0.1 M) at a scanning rate of 40 mV/s by using Ag/AgCl as reference electrode. The HOMO levels were estimated from the following equation $E_{HOMO} = E_p + 4.38$ eV, where E_p represents the onset potential for oxidation relative to the Ag/AgCl reference elecgtrode.[16] The properties of all the fabricated OTFT devices were evaluated using a Keithley SCS-4200 characterization system in ambient conditions.

Synthesis. All the chemicals were purchased from Sigma-Aldrich and used without further purification. Thieno[3,2-*b*]-thiophene-2-carboxylic acid **1** was synthesized according to the synthetic method described in the literature.[12] 2,2′-Bithiophene **4** and 2-[2-(4-pentylphenyl)vinyl]-4,4,5,5-tetramethyl-1,3,2-dioxaborolane **6** were obtained from Sigma-Aldrich.

Thieno(3,2-b)thiophene **2**. To a mixture of thieno[3,2-*b*]thiophene-2-carboxylic acid **1** (8.80 g, 47.78 mmol) and copper powder (1.76 g, 27.78 mmol) in a 3-necked flask was added 90 mL of quinoline. The mixture was heated to reflux with stirring for 50 min and then cooled to room temperature. The reaction mixture was diluted with ethyl ether (~300 mL) and filtered to remove solid contents. The organic solution was washed four times with aqueous HCl solution (5%) and 3 times with water, dried with anhydrous magnesium sulfate and filtered. The crude product, obtained after evaporation of the solvents, was purified through column chromatograph on silica gel using hexane as an eluent, and then recrystallized from 2-propanol, providing 5.5 g (yield: 82%) of thieno(3,2-*b*)thiophene **2** as a white crystalline product. ^{1}H NMR ($CDCl_3$, 300 MHz, ppm): δ 7.28 (d, J = 5.1 Hz, 2H), 7.41 (d, J = 5.1 Hz, 2H).

2,5-Dibromothieno (3,2-b) Thiophene **3**. To a stirred solution of thieno(3,2-*b*)thiophene **2** (1.513 g, 10.8 mmol) in a mixture of 25 mL of dichloromethane (CH_2Cl_2) and 12 mL of acetic acid (AcOH) in a 250 mL flask was slowly added NBS (3.84 g, 21.6 mmol) in small portions over a period of 40 min. After the addition, the mixture was stirred at room temperature for 3 h until TLC showed no starting material left. The mixture was washed twice with aqueous $NaHCO_3$ solution (5%) and three times with water, dried with anhydrous magnesium sulfate, and filtered. The product was obtained after evaporation of the solvent and dried in vacuo, resulting in 3.10 g (yield: 96%) of **3** as white solid. ^{1}H NMR ($CDCl_3$, 300 MHz, ppm): δ 7.18 (s, 2H).

2,5-Dibromothiophene **5**. To a stirred solution of 2,2′-bithiophene **4** (10.00 g, 60.15 mmol) in a mixture of 100 mL of dichloromethane (CH_2Cl_2) and 50 of acetic acid (AcOH) in a 500 mL reaction flask was slowly added NBS (22.48 g, 126.30 mmol) in small portions over a period of 30 min. After the addition, the mixture was stirred at room temperature for 3 h. The solid formed during the reaction was collected by filtration, washed with distilled water, rinsed with methanol, and dried in vacuo overnight, providing 17.93 g of **5** as white flakes. Yield: 92%. ^{1}H NMR ($CDCl_3$, 300 MHz, ppm): δ 6.96 (d, J = 3.9, 2H), 6.85 (d, J = 3.9 Hz, 2H).

2,5-Bis[2-(4-pentylphenyl)vinyl]-thieno(3,2-b)thiphene **7**. To a stirred solution of *2,5*-dibromothieno(3,2-*b*)thiophene **3** (3.01 g, 10.1 mmol) and 2-[2-(4-pentylphenyl)vinyl]-4,4,5,5,-tetramethyl-1,3,2-dioxaborolane **6** (7.58 g, 25.2 mmol) in 100 mL of toluene, under argon, was added a 2 M aqueous sodium carbonate solution (28 mL), Aliquat 336 (2.02 g, 5.0 mmol) in 25 mL of toluene and tetrakis(triphenylphosphine)palladium(0) (0.23 g, 0.20 mmol). The mixture was heated to 90 °C and refluxed at this temperature

(16) Li, Y.; Ding, J.; Day, M.; Tao, Y.; Lu, J.; D'iorio, M. *Chem. Mater.* **2004**, *16*, 2165.

for three days. The precipitated solid product was collected by filtration and washed with methanol. The crude product was recrystallized three times in a mixture of toluene and chlorobenzene at a ratio of three to one by volume, providing 3.57 g (yield: 73%) of 2,5-bis[2-(4-pentylphenyl)vinyl]-thieno(3,2-b)thiophene **7** as a shiny yellowish crystal. Mass spectra analysis: 484.2259 ($C_{32}H_{36}S_2$ calculated 484.2258). Melting point: 320.5 °C. Elemental anal. Calcd for $C_{32}H_{36}S_2$: C, 79.29; H, 7.47; S, 13.23. Found: C, 78.73; H, 7.49; S, 13.00. ^{1}H NMR ($CDCl_3$, 300 MHz, ppm): δ 7.32 (dd, $J = 8.1$ Hz, 4H), 7.13 (dd, $J = 8.1$ Hz, 4H), 7.12 (s, 2H), 7.04 (br, 2H), 6.90 (br, 2H), 2.58 (t, $J = 7.2$ Hz, 4H), 1.61 (m, 4H), 1.32 (m, 8H), 0.90 (t, $J = 6.0$ Hz, 6H).

2,5-Bis[2-(4-pentylphenyl)vinyl]-2,2′-bithiophene ***8***. To a stirred solution of *2,5*-dibromothiophene **5** (3.25 g, 10.0 mmol) and 2-[2-(4-pentylphenyl)vinyl]-4,4,5,5,-tetramethyl-1,3,2-dioxaborolane **6** (7.51 g, 25.0 mmol) in 100 mL of toluene under argon was added 2 M aqueous sodium carbonate solution (28 mL), Aliquat 336 (2.02 g, 5.0 mmol), in 25 mL of toluene and tetrakis(triphenylphosphine)palladium(0)(0.23 g, 0.20 mmol). The resulting mixture was heated to 90 °C and refluxed at this temperature for 3 days. The resulting precipitated solid was collected by filtration and washed with methanol. Additional product was collected from the filtrate, which was washed with water, extracted with toluene, dried with $MgSO_4$, and filtered. The combined crude product was recrystallized from a mixture of toluene and chlorobenzene at a ratio of three to one by volume, providing 3.4 g (yield: 66%) of 2,5-bis[2-(4-pentylphenyl)vinyl]-2,2'-bithiophene **8** as shiny orange crystals. Mass spectra analysis: 510.2411 ($C_{34}H_{38}S_2$ calculated 510.2415); Melting point: 214.39 °C; Elemental anal. Calcd for $C_{34}H_{38}S_2$: C, 79.95; H, 7.50; S, 12.55. Found: (C, 78.99, 7.27, 12.29). ^{1}H NMR ($CDCl_3$, 300 MHz, ppm): δ 7.38 (dd, $J = 8.1$ Hz, 4H), 7.16 (dd, $J = 8.1$ Hz, 4H), 7.13 (d, $J = 15.9$ Hz, 2H), 7.06 (d, $J = 3.9$ Hz, 2H), 6.94 (d, $J = 3.9$ Hz, 2H), 6.87 (d, $J = 15.9$ Hz, 2H), 2.60 (t, $J = 7.5$ Hz, 4H), 1.62 (m, 4H), 1.33 (m, 8H), 0.89 (t, $J = 6.9$ Hz, 6H).

OTFT Fabrication and Evaluation. Both top-contact and bottom-contact thin film transistors using compounds **7** and **8** as channel semiconductor were fabricated. Devices were built on an n-doped silicon wafer with a thermally grown silicon oxide layer (SiO_2, $\sim$ 100 nm). The silicon wafer acted as the gate electrode and the SiO_2 layer acted as gate dielectric. The wafer was cleaned with isopropanol, argon plasma, isopropanol, and dried with air. The wafer was then immersed in a 0.1 M solution of octyltrichlorosilane, OTS-8, in toluene at 60 °C for 20 min. The modified wafer was then washed with toluene, isopropanol, and air-dried. For top-contact devices a 100 nm thick semiconductor layer of compound **7** (or **8**) was vacuum-deposited on the OTS-8 treated silicon wafer substrate at a rate of 1 Å/s under a high vacuum of 1×10^{-6} torr with the substrate held at various temperatures. The gold source and drain electrodes were deposited on top of the semiconductor layer by vacuum deposition through a shadow mask with various channel lengths and widths, creating a series of OTFT transistors with various channel length (L) and width (W) dimensions. For bottom-contact device, gold electrodes were deposited through shadow mask first on OTS-8 modified silicon wafer, followed by modification with octanethiol. A semiconductor layer was subsequently deposited to complete the devices. The properties of the OTFT devices fabricated with compound **7** and **8** as channel semiconductor materials were evaluated using a Keithley 4200 SCS semiconductor characterization system at ambient conditions. Their field-effect mobility, μ, was calculated from the data in the saturated regime according to the following equation: $I_{SD} = C_i\mu(W/2L)(V_G - V_T)^2$, where I_{SD} is the source drain current at the saturated regime, W and L are the width and length of the semiconductor channel, respectively, C_i is the capacitance per unit area of the gate dielectric layer, and V_G and V_T are the gated voltage and threshold voltage, respectively. V_T of the device was determined from the relationship between the square root of I_{SD} at the saturated regime and V_G was obtained by extrapolating the measured data to $I_{SD} = 0$. Devices were kept in the dark in a humidity control chamber (RH $<$ 30%) for stability testing.

Acknowledgment. We thank Dr. Jim Britten in the Chemistry Department at McMaster University for single-crystal X-ray diffraction characterization.

Supporting Information Available: The cif file of single-crystal **8**, cyclic voltammetric curves of **7** and **8**, and transfer curves over time of a top-contact device with **7** (PDF). This material is available free of charge via the Internet at http://pubs.acs.org.